

**Zeitschrift:** IABSE publications = Mémoires AIPC = IVBH Abhandlungen  
**Band:** 31 (1971)  
  
**Artikel:** Ultimate strength and design of reinforced concrete beams in torsion and bending  
**Autor:** Lampert, Paul / Thürlimann, Bruno  
**DOI:** <https://doi.org/10.5169/seals-24211>

### **Nutzungsbedingungen**

Die ETH-Bibliothek ist die Anbieterin der digitalisierten Zeitschriften auf E-Periodica. Sie besitzt keine Urheberrechte an den Zeitschriften und ist nicht verantwortlich für deren Inhalte. Die Rechte liegen in der Regel bei den Herausgebern beziehungsweise den externen Rechteinhabern. Das Veröffentlichen von Bildern in Print- und Online-Publikationen sowie auf Social Media-Kanälen oder Webseiten ist nur mit vorheriger Genehmigung der Rechteinhaber erlaubt. [Mehr erfahren](#)

### **Conditions d'utilisation**

L'ETH Library est le fournisseur des revues numérisées. Elle ne détient aucun droit d'auteur sur les revues et n'est pas responsable de leur contenu. En règle générale, les droits sont détenus par les éditeurs ou les détenteurs de droits externes. La reproduction d'images dans des publications imprimées ou en ligne ainsi que sur des canaux de médias sociaux ou des sites web n'est autorisée qu'avec l'accord préalable des détenteurs des droits. [En savoir plus](#)

### **Terms of use**

The ETH Library is the provider of the digitised journals. It does not own any copyrights to the journals and is not responsible for their content. The rights usually lie with the publishers or the external rights holders. Publishing images in print and online publications, as well as on social media channels or websites, is only permitted with the prior consent of the rights holders. [Find out more](#)

**Download PDF:** 30.12.2025

**ETH-Bibliothek Zürich, E-Periodica, <https://www.e-periodica.ch>**

# **Ultimate Strength and Design of Reinforced Concrete Beams in Torsion and Bending**

*Résistance et dimensionnement des poutres en béton armé soumises à la torsion et à la flexion*

*Bruchwiderstand und Bemessung von Stahlbetonbalken unter Torsion und Biegung*

PAUL LAMPERT

Dr. sc. techn.

BRUNO THÜRLIMANN

Prof. Dr.

Institute of Structural Engineering, Swiss Federal Institute of Technology (ETH)  
Zurich (Switzerland)

## **1. Introduction**

Since about ten years experimental and theoretical research into the behavior of reinforced and prestressed concrete beams subjected to torsion and combined torsion-bending-shear has been intensified world wide (see e.g. [9]). For the past seven years such a program has been under way at the Institute of Structural Engineering, Swiss Federal Institute of Technology, Zurich. The aim of the project is to develop a failure model for reinforced and prestressed concrete beams applicable to general cross sectional shapes including on one side small solid sections used in buildings, on the other side large sections such as box sections occurring in prestressed concrete bridges. Results of the experimental and theoretical studies have been reported in references [1] to [5].

In the present paper a failure model in the form of a space truss is presented and applied to the case of combined torsion and bending. Its validity has been confirmed by an extensive series of tests. Part of the resulting design provisions have already been accepted in the revision of the CEB-Recommendations (Comité Européen du Béton) [7]. At present further studies are made to include in the theoretical approach the influence of shear.

## 2. Ultimate Strength

### 2.1. Failure Model

A general failure model was developed in [5] (see Fig. 1). This space truss model consists of longitudinal reinforcement considered to be concentrated into stringers at the corners and intermediate shear walls. In these shear walls stirrups act as posts and the concrete between the inclined cracks provides the compression diagonals. The angle of the diagonals with respect to the

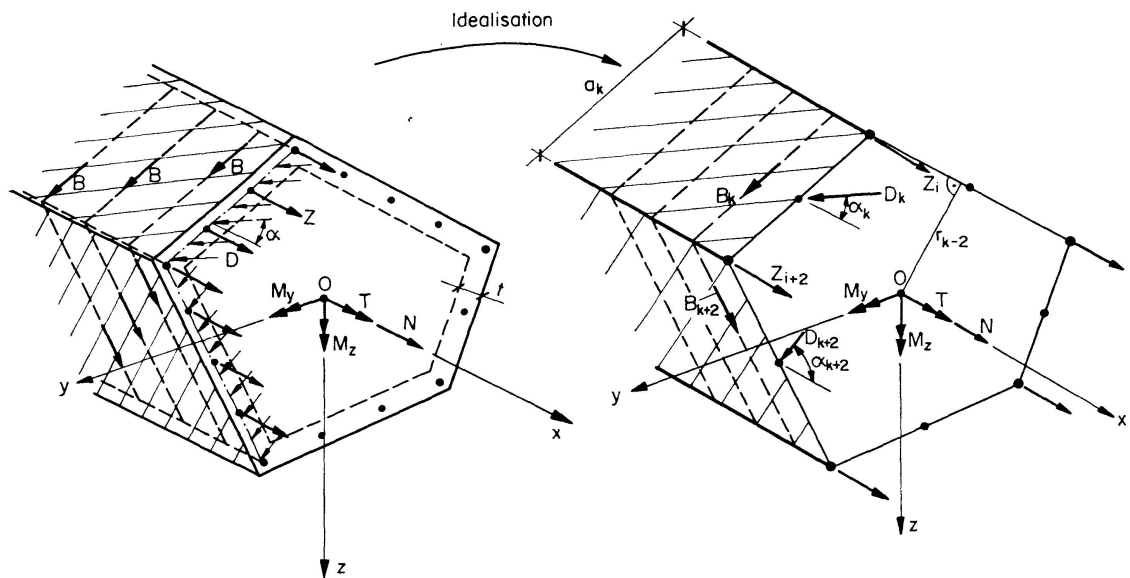


Fig. 1: Failure Model - Space Truss with Variable Inclination of the Diagonals

beam axis is taken to be constant for each side. The angle is such that in the walls governing the failure, both the longitudinal and stirrup reinforcement will reach their yield stresses. For this reason the model is a space truss with variable inclination of the diagonals.

The model can be applied in the case of St. Venant's torsion to the complete range of interaction between general bending, axial force and torsion. The limitations of application and the detailing of the reinforcement will be discussed in Chapter 3. Since a concrete failure is excluded through the assumption of an under-reinforced section, the failure is determined by the yield forces of the longitudinal stringers and the stirrups. Thus it is possible to investigate the failure model by means of the upper and lower bound theorems of the Theory of Plasticity. For this purpose an idealized elastic-plastic stress-strain curve for the reinforcing steel is assumed and equilibrium is formulated for the undeformed system (first order theory). The application to rectangular reinforced concrete beams under torsion will be demonstrated next.

## 2.2. Rectangular Cross Section in Pure Torsion

### 2.2.1. Lower Bound Solution

According to the lower bound (or static) theorem (e.g. [6]), any load for which a stable, statically admissible state of stress exists, will be smaller than or equal to the collapse load. Hence, the forces in the longitudinal reinforcement, stirrups and concrete compression diagonals must be in equilibrium with the applied torque. The forces in the reinforcements cannot exceed the yield forces (yield condition). It is presupposed that the amount of reinforcement is such that the concrete compression diagonals will not crush prior to collapse (under-reinforced members).

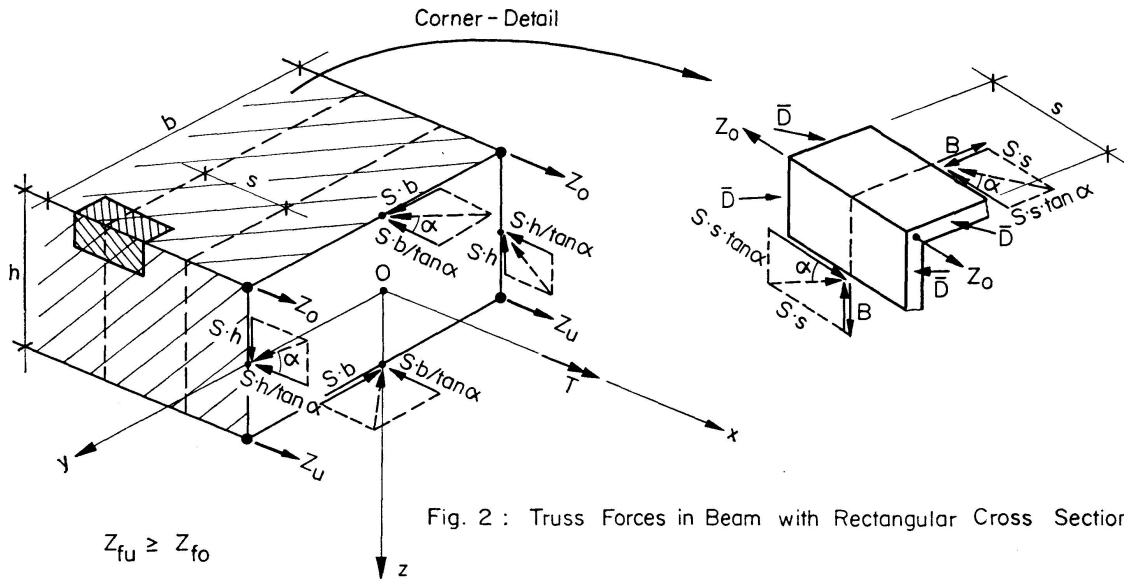


Fig. 2 : Truss Forces in Beam with Rectangular Cross Section

The forces acting in a cross section normal to the beam axis are shown in Fig. 2. The cross section is considered to be symmetrical about the  $z$ -axis. The stirrup reinforcement is taken to be constant on all sides. In the corner detail it can be seen by resolving the forces in the  $x$ -direction that the shear flow  $S$  must be constant around the whole perimeter. Equilibrium in the  $y$ - and  $z$ -directions gives

$$B = S s \tan \alpha. \quad (1)$$

Consider a mechanism produced by yielding of the stirrups. The yield force of one stirrup is  $B_f$ . Because the stirrup reinforcement is constant, the same angle

$$\tan \alpha = \frac{B_f}{S s} \quad (2)$$

occurs on every side. Fig. 2 already shows this inclination and the shear flow as constant. The three of the six equilibrium conditions remaining are



$$\sum X = 0 = 2(Z_o + Z_u) - 2 \frac{S}{\tan \alpha} (b + h), \quad (3)$$

$$\sum M_y = 0 = 2(Z_u - Z_o) \frac{h}{2}, \quad (4)$$

$$\sum M_x = T = (Sb)h + (Sh)b = 2F_0 S. \quad (5)$$

The last Eq. (5) is otherwise known in the form  $S = \tau t = T/2 F_0$  for hollow, thin-walled sections. The area  $F_0$  is defined as the area enclosed by the line connecting the longitudinal reinforcement in the corners [4].

If one assumes that the yield force for the bottom longitudinal reinforcement is larger than for the top longitudinal reinforcement ( $Z_{fu} \geq Z_{fo}$ ) then the top reinforcement will reach its yield stress as a result of the condition given by Eq. (4). Substituting  $Z_u = Z_{fo}$  from Eq. (4) and  $u = 2(b + h)$  into Eq. (3) gives for yielding of the longitudinal reinforcement:

$$4 Z_{fo} = \frac{S u}{\tan \alpha}$$

substituting for  $S$  in Eq. (5)

$$T(L) = \frac{8 F_0}{u} Z_{fo} \tan \alpha. \quad (6)$$

In the case of yielding of the stirrups Eq. (2) and (5) give the corresponding torque

$$T(B) = \frac{2 F_0}{s} \frac{B_f}{\tan \alpha}. \quad (7)$$

Equating the two torques  $T(L)$  and  $T(B)$  results in the condition for the inclination of the compression diagonals  $\alpha$ :

$$\tan^2 \alpha = \frac{B_f}{s} \frac{u}{4 Z_{fo}}. \quad (8)$$

Combining the Eq. (8) and (6) or (7) yields the ultimate torque in the case of pure torsion

$$T_{u0} = 2 F_0 \sqrt{\frac{B_f}{s} \frac{4 Z_{fo}}{u}}. \quad (9)$$

Because  $Z_{fu} \geq Z_{fo}$  and  $Z_u = Z_{fo}$  (Eq. (4))  $Z_u$  is always less than or equal to  $Z_{fu}$ . Accordingly the yield condition is not violated. Thus  $T_{u0}$  as in Eq. (9) is a lower bound value.  $T_{u0}$  will be the exact collapse torque, if it can also be shown that a collapse mechanism will be formed. This will be demonstrated in the following section.

In the special case of the longitudinal reinforcement being uniformly distributed on the perimeter ( $Z_{fu} = Z_{fo}$ ) and stirrup and longitudinal reinforcement being of equal volume ( $4 Z_{fo} s = B_f u$ ) the value  $\tan \alpha$  will be 1 (Eq. (8)) and from Eq. (9)

$$T_{u0}(\tan \alpha = 1) = 2 F_0 \frac{B_f}{s} = 2 F_0 \frac{4 Z_{fo}}{u}. \quad (10)$$

A similar expression has been derived by Moersch more than fifty years ago.

### 2.2.2. Upper Bound Solution

By the upper bound (or kinematic) theorem (e.g. [6]), any load for which there exists an unstable, kinematically admissible state of motion, will be larger than or equal to the collapse load. Thus the deformations of the longitudinal and stirrup reinforcement must be compatible and the rate of work of the applied torque in the collapse mechanism must be equal to the rate of dissipation of energy by the yield forces in the reinforcement ( $L_a = L_d$ ).

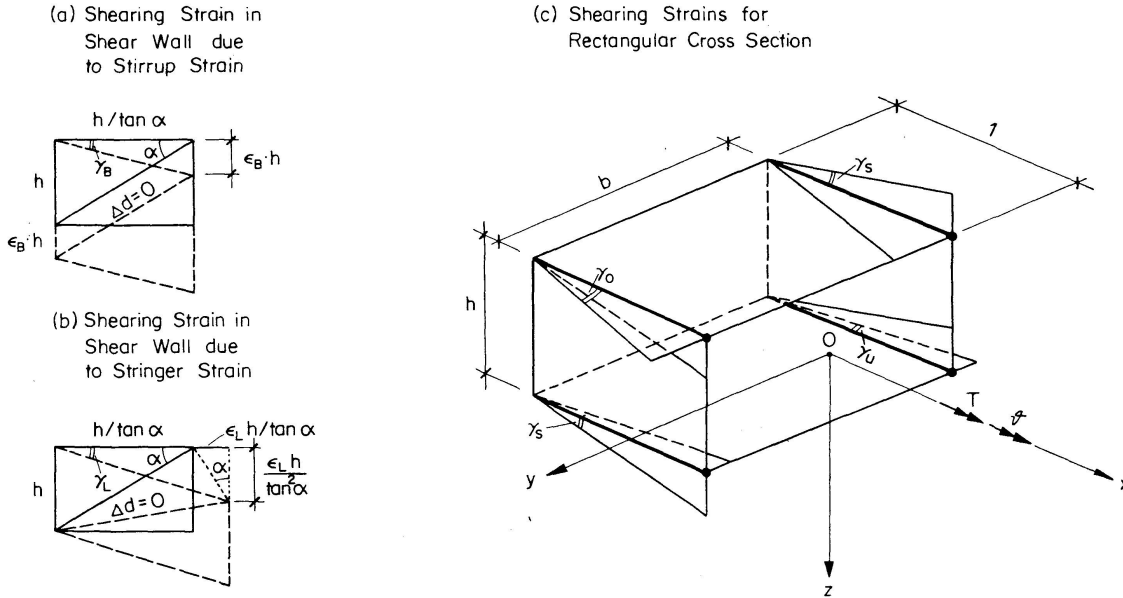


Fig. 3 : Displacement Diagram for a Rectangular Cross Section

The kinematic conditions in a shear wall are shown by means of the displacement diagram in Fig. 3. Basically the shearing strain  $\gamma$  is composed of elongations in the longitudinal and transverse reinforcement and a shortening in the concrete compression diagonals. Since only under-reinforced members are considered, the compression diagonals do not dissipate any energy at failure. Therefore the compression diagonals are assumed to be rigid ( $\Delta d = 0$ ). The shearing strain due to a stirrup strain is obtained directly from the diagram in Fig. 3(a):

$$\gamma_B = \epsilon_B \tan \alpha.$$

Similarly from Fig. 3(b) the shearing strain due to a stringer strain is seen to be

$$\gamma_L = \frac{\epsilon_L}{\tan \alpha}.$$

Thus the total shearing strain is related to the elongation of the reinforcement as follows:

$$\gamma = \gamma_B + \gamma_L = \epsilon_B \tan \alpha + \frac{\epsilon_L}{\tan \alpha}. \quad (11)$$

The relationship between twist and shearing strain is derived in Fig. 4. The angle of twist  $d\vartheta$  is a function of the sum of shearing strains around the perimeter:

$$\frac{d\vartheta}{dx} = \frac{1}{2 F_0} \oint \gamma ds.$$

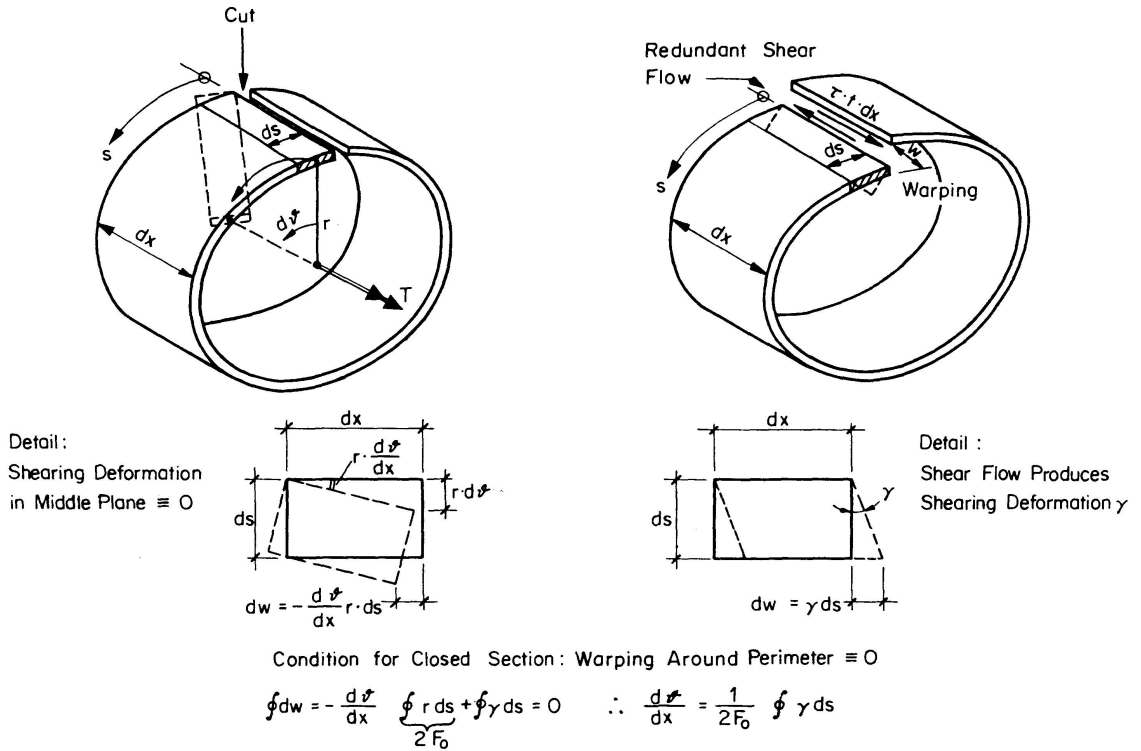


Fig. 4 : Relationship Twist - Shearing Strain for a Thin-Walled Closed Cross Section

For the special case of a rectangular cross section (Fig. 3(c)) the angle of twist  $\vartheta$  per unit length is

$$\vartheta = \frac{1}{2 F_0} [(\gamma_o + \gamma_u) b + 2 \gamma_s h].$$

Herein  $\gamma_o$ ,  $\gamma_u$  and  $\gamma_s$  stand for the shearing strains in the top, bottom and side shear walls, the shearing strains on the sides being equal due to symmetry with respect to the  $z$ -axis. In calculating  $\gamma_s$  with Eq. (11) the stringer strain stands for the average from top and bottom walls and hence:

$$(\gamma_o + \gamma_u) = 2 \gamma_s.$$

Thus the above equation can be simplified:

$$\vartheta = \frac{1}{2 F_0} (\gamma_o + \gamma_u) (b + h) = \frac{u}{4 F_0} (\gamma_o + \gamma_u). \quad (12)$$

By means of Eq. (12) and (11) the rate of work of the applied torque  $L_a$  can now be expressed as:

$$L_a = T \dot{\vartheta} = \frac{T u}{4 F_0} (\dot{\gamma}_o + \dot{\gamma}_u) = \frac{T u}{4 F_0} \left( 2 \dot{\epsilon}_B \tan \alpha + \frac{\dot{\epsilon}_{Lo} + \dot{\epsilon}_{Lu}}{\tan \alpha} \right). \quad (13)$$

The rate of dissipation of energy is given by the product of the yield forces in the reinforcement and the strain rate of the mechanism. It is obtained by summing the separate components of the rates of dissipation of the yield forces in the longitudinal reinforcement,  $Z_{fo}$  and  $Z_{fu}$ , and in the stirrups  $B_f$ :

$$L_d = 2 Z_{fo} \dot{\epsilon}_{Lo} + 2 Z_{fu} \dot{\epsilon}_{Lu} + 2 B_f \frac{1}{s} (b + h) \dot{\epsilon}_B. \quad (14)$$

With the condition that  $L_a = L_d$ , combining Eq. (13) and (14) gives

$$T = \frac{4 F_0}{u} \frac{\left( 2 Z_{fo} \dot{\epsilon}_{Lo} + 2 Z_{fu} \dot{\epsilon}_{Lu} + B_f \frac{u}{s} \dot{\epsilon}_B \right)}{\left( 2 \dot{\epsilon}_B \tan \alpha + \frac{\dot{\epsilon}_{Lo} + \dot{\epsilon}_{Lu}}{\tan \alpha} \right)}. \quad (15)$$

One needs to select that mechanism which gives the least value of the torque as given in Eq. (15). Allowing only one strain rate at a time Eq. (15) gives:

$$T (\dot{\epsilon}_{Lo} \neq 0) = \frac{8 F_0}{u} Z_{fo} \tan \alpha, \quad (16)$$

$$T (\dot{\epsilon}_{Lu} \neq 0) = \frac{8 F_0}{u} Z_{fu} \tan \alpha, \quad (17)$$

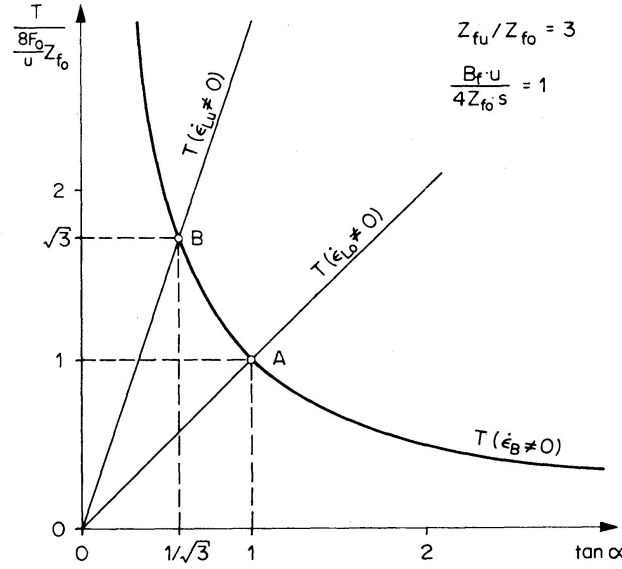
$$T (\dot{\epsilon}_B \neq 0) = \frac{2 F_0 B_f}{s \tan \alpha}. \quad (18)$$

Equating the torque values from Eq. (16) and (18) yields

$$\tan^2 \alpha = \frac{B_f}{s} \frac{u}{4 Z_{fo}},$$

which agrees with Eq. (8). The ultimate torque corresponding to this mechanism is therefore obtained from Eq. (9). Indeed for this mechanism ( $\dot{\epsilon}_{Lo} \neq 0$ ,  $\dot{\epsilon}_B \neq 0$ ) the top longitudinal reinforcement and the stirrups yield. The same assumptions also applied to the derivation of Eq. (9).

The torques from Eq. (16), (17) and (18) are shown graphically in Fig. 5, plotted for  $\frac{Z_{fu}}{Z_{fo}} = 3$  and  $B_f \frac{u}{4 Z_{fo}} s = 1$ . The smaller upper bound for the collapse torque is found at the intersection  $A$ . This mechanism ( $\dot{\epsilon}_{Lo} \neq 0$ ,  $\dot{\epsilon}_B \neq 0$ ) is equivalent to the correct collapse mechanism of the considered model, since the collapse torque agrees with the lower bound value from Eq. (9). The yield condition for this case may be checked with Eq. (17). Indeed, for  $Z_{fu} \geq Z_{fo}$ ,  $Z_u$  is always less or equal to  $Z_{fu}$ .

Fig. 5: Torque as a Function of  $\tan \alpha$  for Different Mechanisms

### 2.3. Rectangular Cross Section in Torsion and Bending

#### 2.3.1. General Interaction

For a rectangular cross section, symmetrical about the  $z$ -axis and with constant stirrup reinforcement (as in Fig. 2), the interaction can be derived from the equilibrium conditions which were derived in section 2.2.1. If one considers the moment about the  $y$ -axis to be  $M_y = M$ , then only the left hand side of Eq. (4), namely  $\sum M_y = M$ , is altered. Substituting the expression for  $T$  from Eq. (5) in Eq. (2) to (4), they can be rewritten as

$$\tan \alpha = \frac{2 F_0 B_f}{T s}, \quad (19)$$

$$Z_o + Z_u = \frac{T u}{4 F_0 \tan \alpha}, \quad (20)$$

$$-Z_o + Z_u = \frac{M}{h}. \quad (21)$$

Summing Eq. (20) and (21) gives in the case of pure bending ( $T=0$ )

$$2 Z_u = \frac{M}{h}.$$

Since for collapse under a positive bending moment the bottom stringers yield (i. e.  $Z_u = Z_{fu}$ ), the ultimate bending moment for pure bending of this model is

$$M_{u0} = 2 Z_{fu} h. \quad (22)$$

The ultimate torque in the case of pure torsion was calculated in section 2.2.1, i.e. Eq. (9)

$$T_{u0} = 2 F_0 \sqrt{\frac{B_f}{s} \frac{4 Z_{fo}}{u}}. \quad (23)$$

In this case the top stringers yield since it is assumed that  $Z_{fu} \geq Z_{fo}$ . Therefore somewhere in the range of combined torsion and bending there must be a change from yielding of the bottom to yielding of the top reinforcement. Consequently, these two cases will be considered separately.

For yielding of the bottom reinforcement  $Z_u = Z_{fu}$ . Adding Eq. (20) and (21) and substituting for  $\tan \alpha$  from Eq. (19) yields

$$2 Z_{fu} = \frac{T_u^2}{4 F_0^2} \frac{u s}{2 B_f} + \frac{M_u}{h}.$$

Dividing by  $2 Z_{fu}$  and introducing the ultimate moments for pure bending and pure torsion from Eq. (22) and (23) the following expression is obtained:

$$1 = \frac{T_u^2}{T_{u0}^2} \frac{Z_{fo}}{Z_{fu}} + \frac{M_u}{M_{u0}}.$$

It can be rewritten as

$$\left( \frac{T_u}{T_{u0}} \right)^2 = \frac{Z_{fu}}{Z_{fo}} \left( 1 - \frac{M_u}{M_{u0}} \right). \quad (24)$$

For yielding of the top reinforcement  $Z_o = Z_{fo}$ . In this case subtracting Eq. (21) from Eq. (20), and substituting for  $\tan \alpha$  from Eq. (19) gives:

$$2 Z_{fo} = \frac{T_u^2}{4 F_0^2} \frac{u s}{2 B_f} - \frac{M_u}{h}.$$

Dividing by  $2 Z_{fo}$  and introducing the ultimate moments from Eq. (22) and (23) yields

$$1 = \frac{T_u^2}{T_{u0}^2} - \frac{M_u}{M_{u0}} \frac{Z_{fu}}{Z_{fo}},$$

otherwise

$$\left( \frac{T_u}{T_{u0}} \right)^2 = 1 + \frac{Z_{fu}}{Z_{fo}} \frac{M_u}{M_{u0}}. \quad (25)$$

On the basis of these two equations interaction curves for  $Z_{fu}/Z_{fo} = 3$  and 1 are shown in Fig. (6). It is seen that for a section reinforced for bending ( $Z_{fu} > Z_{fo}$ ), the torsional strength can be increased by the simultaneous application of a bending moment. The maximum torsional strength is given by the intersection *A* of the two curves representing Eq. (24) and (25), at which all the reinforcements of the section yield. For a section reinforced for pure torsion ( $Z_{fu} = Z_{fo}$ ), the maximum torque occurs when the bending moment  $M = 0$ . In this case both the top and bottom longitudinal reinforcement and the stirrups yield. The form of these curves for the interaction between torsion and bending was confirmed by tests [4], [5].

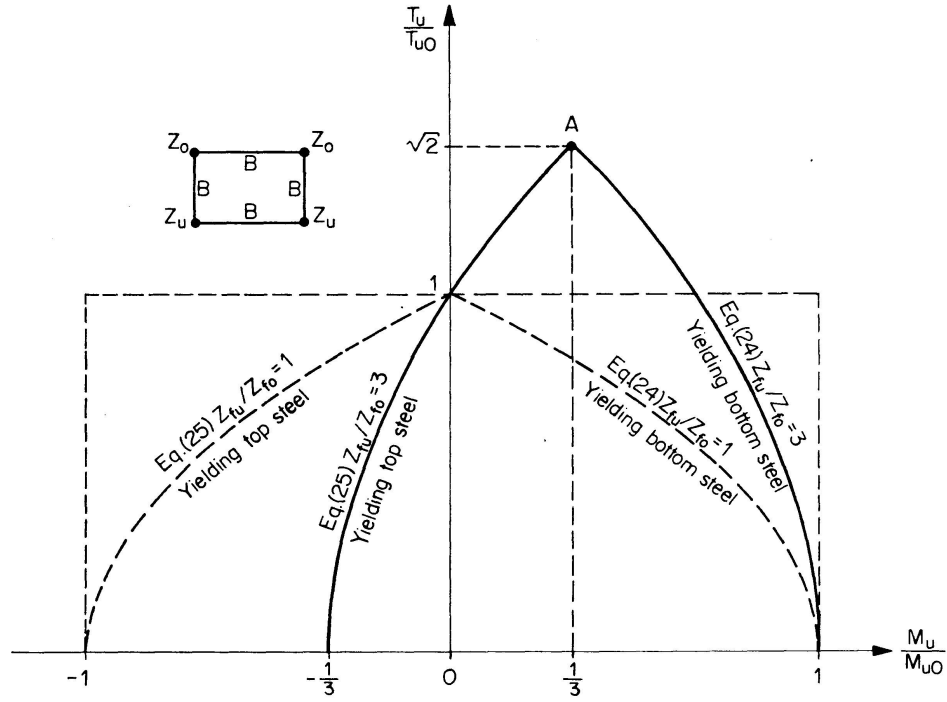


Fig. 6: Interaction Torsion - Bending for a Rectangular Cross Section

### 2.3.2. Ultimate Strength

The following relationships are derived for the case of yielding of the bottom stringers. If for a given torque  $T$  a bending moment  $M_u$  is required Eq. (24) gives

$$M_u = M_{u0} \left[ 1 - \frac{Z_{fo}}{Z_{fu}} \left( \frac{T}{T_{u0}} \right)^2 \right]. \quad (26)$$

For the solution of Eq. (26) one needs the ultimate strength for pure torsion  $T_{u0}$  as given by Eq. (9).

In the case of proportional loading defined by the factor  $\kappa = T/M$ , addition of Eq. (20) and (21) leads to

$$2 Z_{fu} = M_u(\kappa) \left( \frac{\kappa u}{4 F_0 \tan \alpha} + \frac{1}{h} \right),$$

which with  $M_{u0}$  from Eq. (22) gives

$$M_u(\kappa) = \frac{M_{u0}}{1 + \frac{\kappa u h}{4 F_0 \tan \alpha}}. \quad (27)$$

By substituting for  $\tan \alpha$  from Eq. (19) and writing  $T_u(\kappa) = \kappa M_u(\kappa)$ , a quadratic equation for  $M_u(\kappa)$  is obtained:

$$\frac{\kappa^2 u h s}{8 F_0^2 B_f} M_u^2(\kappa) + M_u(\kappa) - M_{u0} = 0.$$

Solving for the ultimate flexural strength gives

$$M_u(\kappa) = \frac{4 F_0^2 B_f}{\kappa^2 u h s} \left( -1 + \sqrt{1 + 4 M_{u0} \frac{\kappa^2 u h s}{8 F_0^2 B_f}} \right). \quad (28)$$

If  $\kappa$  is small, the square root can be expanded into a series

$$\sqrt{1 + \epsilon} = 1 + \frac{\epsilon}{2} - \frac{\epsilon^2}{8} \dots$$

to find the ultimate flexural strength in the vicinity of  $M_{u0}$ :

$$M_u(\kappa)_{\kappa \rightarrow 0} = M_{u0} \left( 1 - \frac{M_{u0} u s}{8 B_f b F_0} \kappa^2 \right). \quad (29)$$

Similar relationships can be derived in the case of the top longitudinal reinforcement yielding, as in [5]. Eq. (27) can alternatively be derived from a kinematic procedure as in section 2.2.2, when the rate of work of the applied moments as given by Eq. (13) is increased by the amount

$$M \dot{\varphi} = M \frac{(\dot{\epsilon}_{Lu} - \dot{\epsilon}_{Lo})}{h}.$$

In the case of the bottom reinforcement yielding ( $\dot{\epsilon}_{Lu} \neq 0$ ) Eq. (13) becomes

$$L_a = \frac{T u}{4 F_0 \tan \alpha} + \frac{M}{h} \dot{\epsilon}_{Lu}$$

and Eq. (14)

$$L_d = 2 Z_{fu} \dot{\epsilon}_{Lu}.$$

Equating  $L_a$  and  $L_d$  and writing  $T = \kappa M$  yields the same expression for  $M_u(\kappa)$  as Eq. (27).

#### 2.4. General Cross Sections

By means of the Theory of Plasticity the failure model for general cross sections (Fig. 1) was investigated in [5]. A linear program can be derived from the equilibrium and the yield conditions. Its maximum value is a lower bound solution for the collapse load (lower bound theorem). Similarly, with the conditions of kinematical compatibility and the equation for the rate of work of the applied and internal forces, a linear program can be found for which the minimum value forms an upper bound solution for the collapse load (upper bound theorem). Since each program is the dual of the other, they both arrive at the same optimum value, namely the exact collapse load for this failure model.

The following basic conclusions have been deduced from this method of solution [5]:



- a) A collapse mechanism opens about a straight line connecting two stringers. As long as this straight line does not intersect the cross section it is a possible axis of rotation for the mechanism (see Fig. 7).
- b) In a collapse mechanism the stirrups yield on all sides of the cross section.

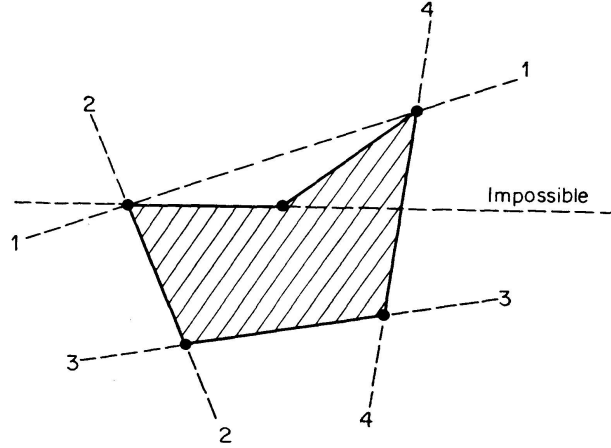


Fig. 7: Possible Axes of Rotation for Failure Model

Combining these two statements is to say that in a collapse mechanism all the stirrups and longitudinal reinforcement reach their yield stresses, with the exception of the two stringers defining the axis of rotation. This statement forms the basis of the general solution.

The 6 equations of equilibrium (compare with Fig. 1 and see reference [5]) are

$$N = \sum_1^m Z_i - \sum_2^n D_k \cos \alpha_k, \quad (30)$$

$$M_y = \sum_1^m Z_i z_i - \sum_2^n D_k \cos \alpha_k z_k, \quad (31)$$

$$M_z = -\sum_1^m Z_i y_i + \sum_2^n D_k \cos \alpha_k y_k \quad (32)$$

$$T = \sum_2^n D_k \sin \alpha_k r_k, \quad (33)$$

$$D_k = S \frac{a_k}{\sin \alpha_k}, \quad (34)$$

$$\tan \alpha_k = \frac{B_k}{S s_k}. \quad (35)$$

Substituting Eq. (34) and (35) in Eq. (30) to (33) and introducing the constant shear flow  $S$ , gives the four essential equations of equilibrium

$$N = \sum_1^m Z_i - S^2 \sum_2^n \frac{a_k s_k}{B_k}, \quad (36)$$

$$M_y = \sum_1^m Z_i z_i - S^2 \sum_2^n \frac{a_k s_k}{B_k} z_k, \quad (37)$$

$$M_z = -\sum_1^m Z_i y_i + S^2 \sum_2^n \frac{a_k s_k}{B_k} y_k, \quad (38)$$

$$T = S \sum_2^n a_k r_k = 2 F_o S. \quad (39)$$

Due to the preceding conclusions a) and b), these relationships have as unknowns, besides the shear flow  $S$  and the ultimate moment  $M_y$  (for a given proportional loading), only the forces in the two stringers defining the axis of rotation. These two stringers will not yield. For all other  $Z_i$  and  $B_k$ , the yield forces  $Z_{fi}$  and  $B_{fk}$  can be substituted, whereby the solution is obtained.

In practice, it is advantageous to place the  $(y, z)$  coordinate axes so that the unknown forces in the stringers which do not yield have a zero lever arm. Thus the ultimate moment  $M_y$ , for example, can be directly calculated from Eq. (37) substituting  $S$  with Eq. (39). The Eq. (36) and (37) are needed only to check the yield conditions. Similarly the interaction diagram can be derived by determining the interaction curves corresponding to all the theoretically possible axes of rotation (Fig. 7). All these curves envelop the actual interaction for the cross section.

### 3. Additional Considerations

#### 3.1. Concrete Failure

In section 2.1 it was assumed that only under-reinforced beams would be considered. In such members the stirrups and longitudinal reinforcement yield prior to failure of the concrete. Concrete failure before yielding of the reinforcement can be caused by

- a) crushing of the concrete compression diagonals;
- b) excessive shearing strains due to a large deviation of the angle  $\alpha$  from  $45^\circ$ ;
- c) crushing of the concrete compression zone.

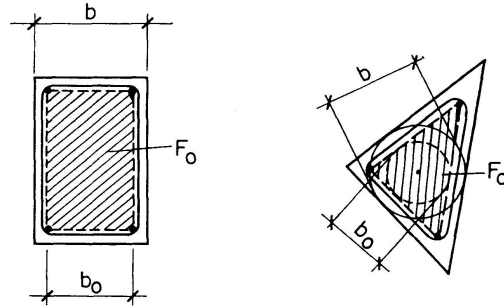
These types of failure are commented upon in the following section, and criteria for their avoidance are proposed.

The concrete compression diagonals carry the diagonal forces necessary for the truss equilibrium in the plane of the reinforcement cage. A beam with a solid cross section has shown essentially the same failure mode as the corresponding hollow section (see references [1] and [2]). Since the core offers no contribution to the torsional strength, it is reasonable to assume an effective outer shell for solid cross sections in computing a nominal shear stress. The thickness of this shell is proposed [4] to be the smaller of the two values

$$t = \frac{b}{6}; \quad t = \frac{b_0}{5}, \quad (40)$$

where  $b$  and  $b_0$  are the diameters of the largest inscribed circles in the cross section and the area  $F_0$  respectively (Fig. 8). The theory of thin-walled box sections gives the shear stress as

$$\tau = \frac{T}{2 F_0 t}. \quad (41)$$



Effective Wall Thickness  $t = b/6$  or  $t = b_0/5$

Fig. 8: Effective Wall Thickness for Solid Cross Sections

For hollow sections  $t$  stands for the actual wall thickness, as long as this is smaller than the effective wall thickness according to Eq. (40). Eq. (34) and (41) give the normal stress in the diagonals as

$$\sigma_D = \frac{-\tau}{\sin \alpha \cos \alpha}. \quad (42)$$

For  $\alpha = 45^\circ$ ,  $\sigma_D = -2\tau$ .

Twisting of a beam induces an additional stress into the diagonals. In reference [1], this was traced to a distortional effect. Through twisting, the originally plane walls of the section are distorted to hyperbolic paraboloids (Fig. 9). The curvature assumes at  $\alpha = 45^\circ$  the maximum value of

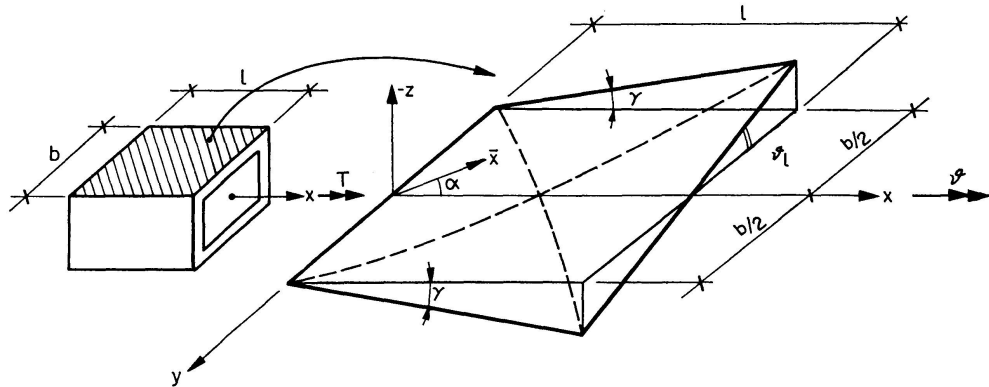


Fig. 9: Distortional Effect

$$\frac{d^2 z}{d\bar{x}^2}(\alpha = 45^\circ) = -\frac{d\vartheta}{dx}. \quad (43)$$

Consequently additional compressive stresses occur on the outer surface of the diagonals, which must be added to those obtained from Eq. (42). Therefore, if one wishes to prevent a crushing failure of the compression diagonals by limiting the maximum shear stress, this stress has to be lower or at least not greater than the maximum permissible shear stress due to a shear force acting on a cross section. This information was used in the revision of the Torsion Provisions in the CEB-Recommendations [7].

The angle  $\alpha$ , characteristic for the redistribution of forces between longitudinal reinforcement and stirrups, is subjected to certain limits. The deviation of  $\alpha$  from  $45^\circ$  depends on the ratio of longitudinal to stirrup reinforcement. Eq. (11)

$$\gamma = \epsilon_B \tan \alpha + \frac{\epsilon_L}{\tan \alpha}$$

shows that the shear strain will be very large for both small and large values of  $\tan \alpha$ . In such cases a concrete failure through excessive shearing can occur before both of the reinforcement components have yielded. Based on the interpretations of the tests in [5], Eq. (35)

$$\tan \alpha_k = \frac{B_k}{S s_k}$$

was used to derive the following limiting values

$$0,5 < \tan \alpha_k < 2,0. \quad (44)$$

Crushing of the concrete compression zone before yielding of the tensile reinforcement can occur by a predominantly flexural loading. However, since a torque always raise the neutral axis as compared with the case of pure bending, the balanced reinforcement leading simultaneously to yielding of the steel and crushing of the concrete in pure bending is at the same time a safe limit for the combined loading.

### 3.2. Cross Sectional Shape

The theory so far is applicable to hollow and solid sections with dimensions of the same order in both directions. Thus the compression diagonals of the truss can develop on the narrower sides as well.

For open cross sections subjected to warping, this theory is only applicable to members in which warping is not restrained by the support or type of loading. In this case the torque is only carried by St. Venant's torsion. In all other cases the warping torsion can be of the same order as the St. Venant's torsion. So far there is no solution for the ultimate strength in this case availa-

ble. It is to be remembered that once cracking has occurred, the torsional stiffness decreases significantly more than the flexural stiffness [2]. This entails a greater influence for warping torsion at ultimate load.

For compound cross sections it must be pointed out that the separate parts rotate about an axis which generally does not coincide with the axes of the individual parts. With variable torsional moments and restrained supports this results in lateral bending of the parts. The corresponding bending moments increase with increasing thickness of the parts. Especially with thick reinforced concrete beams, this contribution can become significant.

### 3.3. Detailing of Reinforcement

In order for the assumed failure model to be applicable, several detailing requirements must be satisfied. So that a trusslike behavior exists on the governing sides of the section, every crack should be crossed by at least one stirrup (Fig. 10). This leads to a minimum stirrup spacing of

$$s \leq \frac{a}{2}, \quad \text{but} \quad s \leq 20 \text{ cm}, \quad (45)$$

where  $a$  is the length of the shortest side. In addition the stirrup reinforcement must be sufficiently anchored on all sides. For shallow rectangular cross sections, common in buildings, a more liberal spacing requirement  $s = \frac{b+h}{4}$  is justified, as proposed in the new ACI-Code [8].

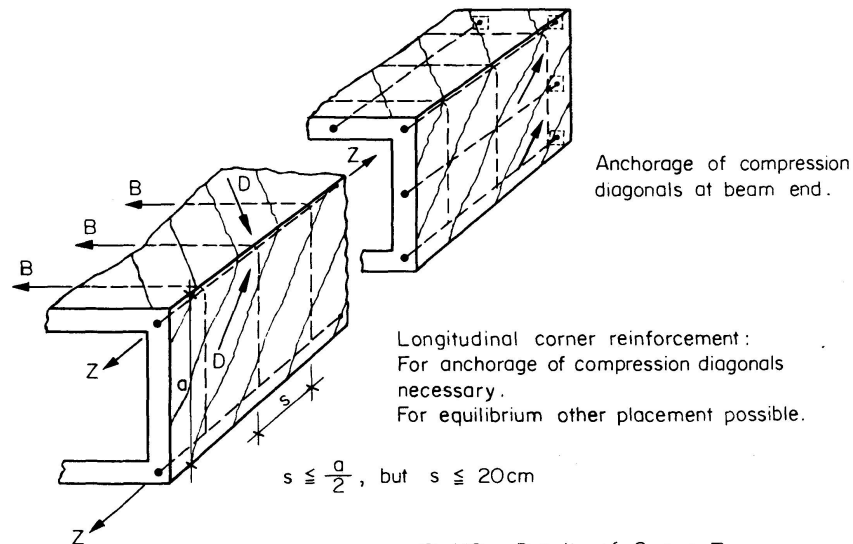


Fig. 10: Details of Space Truss

The absolute limitation of the stirrup spacing to  $s \leq 20 \text{ cm}$  is due to the fact that the stirrups, together with the longitudinal reinforcement in the corners, must prevent the compression diagonals prematurely breaking out between two stirrups. For this reason concentrating the longitudinal reinforce-

ment in the corners of the cross section leads to a favorable deformation behavior, since the corner bars provide a sound support for the diagonals. But in order to avoid too large crack openings, it is an advantage to have some longitudinal reinforcement uniformly distributed over the perimeter. This is also true for locations where a torque is transmitted to the member, for example at the end of a beam, where the diagonals need to be held back by a well anchored and uniformly distributed longitudinal reinforcement (Fig. 10).

It is seen from the corner detail of Fig. 2 and Fig. 10 that for a constant torque the equilibrium conditions do not require the longitudinal reinforcement to be in the corners. Within the beam the longitudinal components of the diagonal forces are self equilibrating, whereas the transverse components must be deviated around the corners by the stirrups. Thus longitudinal reinforcement anywhere in the cross section can be counted on to act as torsional longitudinal reinforcement as well, since it will resist a lengthening of the beam whatever its position.

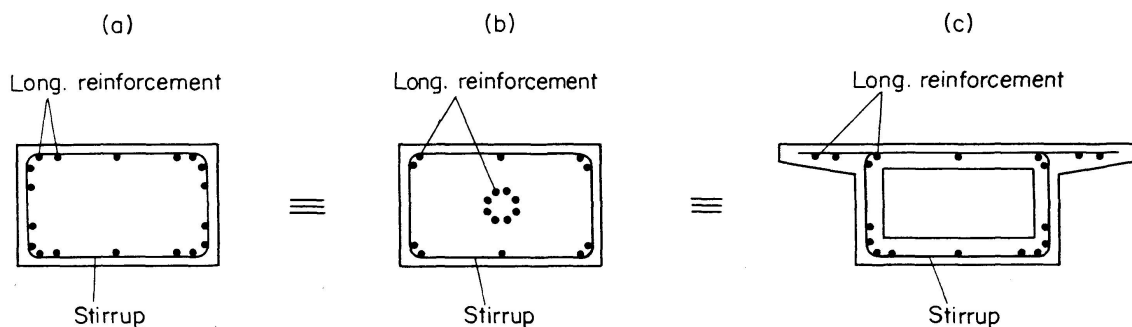


Fig. 11: Distribution of Longitudinal Reinforcement

For example, all the beam sections shown in Fig. 11 have the same ultimate torque, so long as the reinforcement in the corners of 11(b) and 11(c) can anchor the diagonals. The case 11(b) is typical for post-tensioned beams. It should be mentioned that for ultimate strength the prestressed steel can be considered to act as a normal reinforcement [5]. Case 11(c) shows a box section, in which the longitudinal reinforcement outside of the stirrups can be included in the torsional reinforcement as well.

### 3.4. Shape of Concrete Compression Zone

In Fig. 1 the cross section was idealized so that the longitudinal reinforcement was concentrated into stringers at the corners. With a predominantly flexural loading, the stringers on the axis of rotation and the adjacent concrete would be subjected to compression (see Fig. 12(a)). If the center  $D_b$  of the concrete compression zone lies inside the assumed axis of rotation the lever

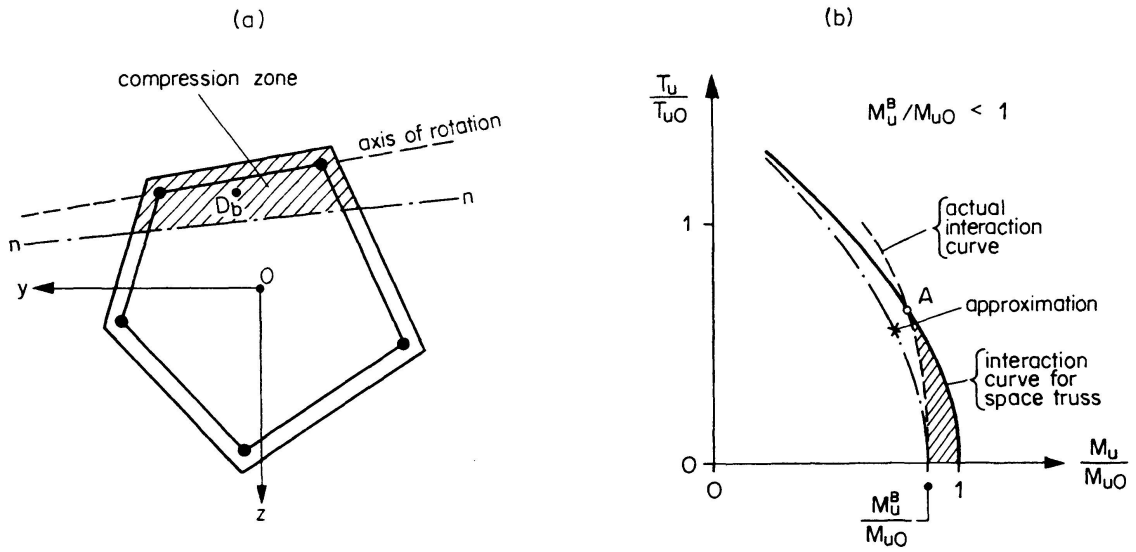


Fig. 12 : Influence of Concrete Compression Zone on Interaction Diagram

arm is reduced and the ultimate moment is less than that for the space truss model.

Since both compressive forces in the stringers on the axis of rotation are known, the value of  $D_b$  can be calculated and for an assumed stress distribution in the concrete (e.g. rectangular stress block), the position of the neutral axis as well [5]. The limiting case is, of course, pure bending, since the addition of a torque always reduces the amount of  $D_b$ .

Fig. 12(b) shows the effect on an interaction diagram. The actual curve has an intercept on the abscissa of  $M_u^B/M_{u0}$ , where  $M_u^B$  is the ultimate moment determined by the simple bending theory. At point A, the resultant  $D_b$  lies exactly on the axis of rotation, which is the center line of the shear wall. In reference [5] it was proposed to divide the ultimate flexural moment  $M_u$  by the smaller of the two values  $M_u^B$  and  $M_{u0}$ . The effect of this approximation is shown in Fig. 12(b).

## 4. Design

### 4.1. Direct Design

The objective is to design the longitudinal and stirrup reinforcement for a given loading and cross section. In the general case, the equilibrium Eq. (34) to (39) are not sufficient to determine the unknown tensile forces  $Z_i$  and  $B_k$  and the angle  $\tan \alpha$ . If in the Eq. (36) to (38) one  $S$  is substituted by means of Eq. (35) the Eq. (34) to (39) read:

$$D_k = S \frac{a_k}{\sin \alpha_k}, \quad (46)$$

$$B_k = S s_k \tan \alpha_k, \quad (47)$$

$$N = \sum_1^m Z_i - S \sum_2^n \frac{a_k}{\tan \alpha_k}, \quad (48)$$

$$M_y = \sum_1^m Z_i z_i - S \sum_2^n \frac{a_k z_k}{\tan \alpha_k}, \quad (49)$$

$$M_z = -\sum_1^m Z_i y_i + S \sum_2^n \frac{a_k y_k}{\tan \alpha_k}, \quad (50)$$

$$T = 2 F_0 S. \quad (51)$$

For assumed values of  $\tan \alpha$  the stirrup reinforcement can be determined from Eq. (47). The Eq. (48), (49) and (50) enable three stringer forces to be calculated. If there are more than three stringers the problem is no longer uniquely defined and hence different solutions are possible.

It will be shown that the volume of torsional reinforcement is a minimum for an angle of  $\tan \alpha = 1$ . The sum of the yield forces in the longitudinal and stirrup reinforcement per unit length can be taken as a measure of the steel volume.

$$Y = \sum_1^m Z_{fi} + \sum_2^n B_{fk} \frac{a_k}{s_k}. \quad (52)$$

With  $Z_i = Z_{fi}$  and  $N = 0$  for the case of torsion only, Eq. (48) gives

$$\sum_1^m Z_{fi} = S \sum_2^n \frac{a_k}{\tan \alpha_k}.$$

Substituting  $B_k = B_{fk} = S s_k \tan \alpha_k$  from Eq. (47) in Eq. (52) for the steel volume gives

$$Y = S \sum_2^n \frac{a_k}{\tan \alpha_k} + S \sum_2^n a_k \tan \alpha_k. \quad (53)$$

If all the derivatives of  $Y$  with respect to  $\alpha_k$  vanish then

$$\frac{dY}{d\alpha_k} = S \left( \frac{-a_k}{\sin^2 \alpha_k} + \frac{a_k}{\cos^2 \alpha_k} \right) = 0,$$

from which, since  $S \neq 0$ , one deduces that

$$\tan \alpha_k (Y_{min}) = 1. \quad (54)$$

It is therefore justified to base the design on a space truss with  $45^\circ$  diagonals. Fig. 13 shows the general relationship between the steel volume  $Y$  and  $\tan \alpha$  after Eq. (53), for  $\tan \alpha$  constant around the perimeter of the section

$$\frac{Y}{S u} = \frac{1}{\tan \alpha} + \tan \alpha. \quad (55)$$

The Eq. (47) to (50) can now be further simplified by putting  $\tan \alpha_k = \text{con-}$



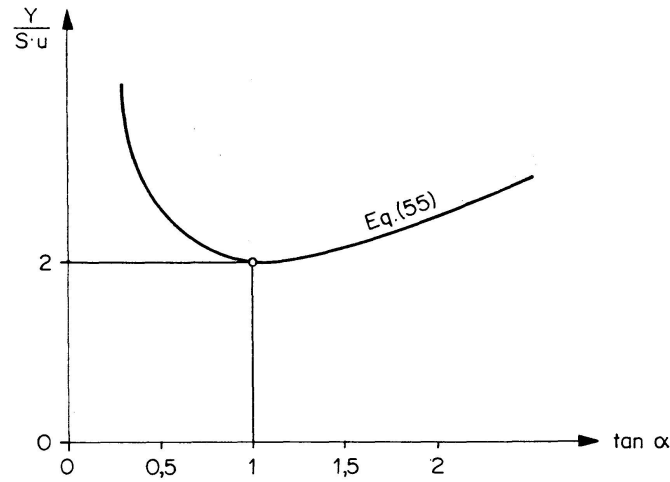


Fig.13 : Minimum Steel Volume

stant = 1 and substituting  $S$  from Eq. (51) to

$$\frac{B_k}{s_k} = \frac{T}{2 F_0}, \quad (56)$$

$$\sum_1^m Z_i = N + \frac{T u}{2 F_0}, \quad (57)$$

$$\sum_1^m Z_i z_i = M_y + \frac{T}{2 F_0} \sum_2^n a_k z_k, \quad (58)$$

$$\sum_1^m Z_i y_i = -M_z + \frac{T}{2 F_0} \sum_2^n a_k y_k. \quad (59)$$

These relationships are valid for general cross sections. It is interesting to note that the stirrup reinforcement is only dependent on the torque.

In the special case of pure torsion Eq. (56) and (57), with  $B_k = \sigma_e F_B$  and  $\sum Z_i = \sigma_e \sum F_L$  and a constant steel quality, lead to the design relationship

$$\frac{F_B}{s} = \frac{\sum F_L}{u} = \frac{T}{2 F_0 \sigma_e}. \quad (60)$$

This equation has been accepted for the CEB recommendations [7].

For a rectangular section in torsion and bending as in Fig. 2 Eq. (59) is eliminated due to symmetry about the  $z$ -axis. If one positions the  $y$ -axis through the top stringers, then Eq. (58) leads directly to

$$2 Z_u h = M + \frac{T}{2 F_0} (b h + h^2)$$

or with  $Z_u = \sigma_e F_u$  the area of the bottom stringers is

$$F_u = \frac{M}{2 h \sigma_e} + \frac{T u}{8 F_0 \sigma_e}. \quad (61)$$

Finally with  $Z_o = \sigma_e F_o$ , Eq. (57) or (60) gives the area of the top stringers

$$F_o = -\frac{M}{2h\sigma_e} + \frac{T u}{8F_o\sigma_e}. \quad (62)$$

Eq. (60) to (62) are applicable for a design based on allowable stress or ultimate strength. In the first case  $M$  and  $T$  are the allowable moment and torque,  $\sigma_e$  the allowable steel stress. In the second case  $M$  and  $T$  are the ultimate moment and torque and  $\sigma_e$  the yield stress of the steel.

Eq. (61) and (62) show that the longitudinal reinforcement is composed of a flexural and a torsional part. It should be noted that the top longitudinal torsional reinforcement in Eq. (62) can be reduced by the term arising from the compressive force due to bending. This superposition of forces is illustrated in Fig. 14. Whereas in the bottom stringers the flexural term is added to the torsional tensile force, it counteracts in the top stringers.

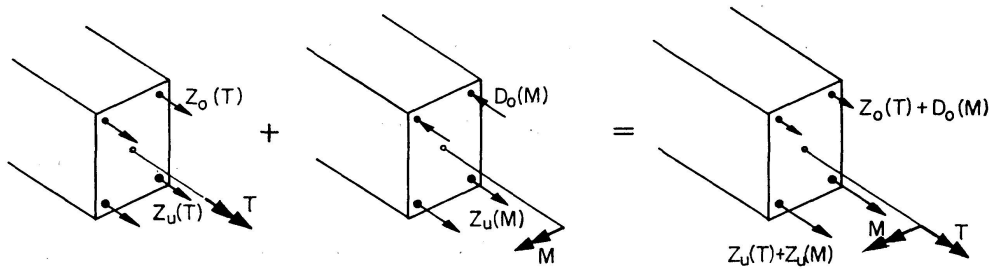


Fig. 14: Superposition of Forces in Longitudinal Reinforcement

The simple procedure of calculating the torsional reinforcement from Eq. (60) or Eq. (57) for the torque and the necessary flexural reinforcement for the bending moment separately and superimposing the two is also applicable to general cross sections. In the tensile zone the two longitudinal steel components are added, whereas in the flexural compression zone the longitudinal torsional reinforcement can be reduced by an amount corresponding to the flexural compressive force. By observing maximum and minimum reinforcement percentages and by limiting the maximum permissible shear stress, a premature concrete failure can be prevented. In addition the reinforcement has to be properly detailed as described in section 3.3.

#### 4.2. Ultimate Strength Check

Instead of a direct design, it is often more expedient to carry out the design indirectly, by checking the ultimate strength. The procedure suggests itself for large and in particular prestressed beams. Box sections of bridges, for example, require a considerable amount of longitudinal and stirrup reinforcement in the webs, and top and bottom slabs due to bending moments and shear forces alone. Consequently they already have a considerable ultimate

torsional strength. The interaction curves, corresponding to Eq. (36) to (38) and Fig. 6 are particularly suitable for a judgement of the torsional behavior if different loading cases have to be considered.

### Notations

#### *Lengths and Areas*

$a$	distance between longitudinal corner bars
$b$	width between longitudinal corner bars
$h$	height between longitudinal corner bars
$r$	distance of shear flow from axis of twist
$s$	stirrup spacing
$t$	wall thickness of (effective) box section
$u$	perimeter of area $F_0$
$x$	coordinate axis in direction of beam axis
$y$	coordinate axis; distance in $y$ -direction
$z$	coordinate axis; distance in $z$ -direction
$F_0$	area enclosed by the line connecting the longitudinal reinforcement in the corners
$F_o, F_u$	area of top resp. bottom longitudinal stringer
$F_B$	area of one stirrup leg
$F_L$	area of one longitudinal stringer
$\sum F_L$	area of all longitudinal reinforcement

#### *Forces and Moments*

$B$	force in one stirrup leg
$B_f$	yield force in one stirrup leg
$D$	resultant force in concrete compression diagonals
$L_a$	rate of work
$L_d$	rate of dissipation of energy
$M$	bending moment
$M_u$	ultimate bending moment
$M_{u0}$	ultimate bending moment for pure bending
$M_u^B$	ultimate moment determined by the bending theory
$N$	axial force
$S$	shear flow
$T$	torque
$T_u$	ultimate torque
$T_{u0}$	ultimate torque for pure torsion
$Z$	force in longitudinal reinforcement
$Z_f$	yield force in longitudinal reinforcement

$Z_o, Z_u$  force in top resp. bottom longitudinal stringer  
 $Z_{fo}, Z_{fu}$  yield force in top resp. bottom longitudinal stringer

### *Stresses*

$\sigma_e$  stress in steel reinforcement  
 $\sigma_D$  stress in concrete diagonal  
 $\tau$  shear stress

### *Deformations, Angles and Parameters*

$\alpha$  angle between concrete diagonal and beam axis  
 $\gamma$  shearing strain  
 $\epsilon$  normal strain  
 $\epsilon_B$  stirrup strain  
 $\epsilon_L$  stringer strain  
 $\vartheta$  angle of twist  
 $\varphi$  curvature  
 $\kappa = T/M$  ratio torque/bending moment

### *Subscripts*

$b$  concrete  
 $e$  steel  
 $f$  yield  
 $i$  number index of corners ( $i$  from 1, 3, 5, ... to  $m$ )  
 $k$  number index of walls ( $k$  from 2, 4, 6, ... to  $n$ )  
 $o$  top  
 $s$  side  
 $u$  bottom, ultimate  
 $x, y, z$  related to  $x$ -,  $y$ -,  $z$ -axis  
 $B$  related to stirrup  
 $D$  related to diagonal  
 $L$  related to longitudinal stringer  
 $0$  zero; pure bending; pure torsion

### **List of References**

1. LAMPERT, P. / THÜRLIMANN, B.: «Torsionsversuche an Stahlbetonbalken.» Bericht Nr. 6506-2, Juni 1968, Institut für Baustatik, ETH Zürich.
2. LAMPERT, P. / THÜRLIMANN, B.: «Torsions-Biege-Versuche an Stahlbetonbalken.» Bericht Nr. 6506-3, Januar 1969, Institut für Baustatik, ETH Zürich.
3. LAMPERT, P. / LÜCHINGER, P. / THÜRLIMANN, B.: «Torsionsversuche an Stahl- und Spannbetonbalken.» Bericht Nr. 6506-4, Februar 1971, Institut für Baustatik, ETH Zürich.

4. LAMPERT, P.: «Torsion und Biegung von Stahlbetonbalken.» Bericht Nr. 27, Januar 1970, Institut für Baustatik, ETH Zürich (Sonderdruck Schweizerische Bauzeitung, 88. Jg., Heft 5, 29. Januar 1970).
5. LAMPERT, P.: «Bruchwiderstand von Stahlbetonbalken unter Torsion und Biegung.» Bericht Nr. 26, Januar 1970, Institut für Baustatik, ETH Zürich (Dissertation Prom. Nr. 4445, 1970, ETH Zürich).
6. THÜRLIMANN, B. / ZIEGLER, H.: «Plastische Berechnungsmethoden.» Eidgenössische Technische Hochschule Zürich, 1963.
7. Comité Européen du Béton: «Recommendations Internationales CEB-FIP pour le Calcul et l'Exécution des Ouvrages en Béton.» 2nd édition, Juin 1970, Cement and Concrete Association, London.
8. ACI 318-71 Building Code Requirements for Reinforced Concrete; American Concrete Institute, Detroit, Mich.
9. "Torsion of Structural Concrete." Journal American Concrete Institute, April 1968, page 310; Publication SP-18.

### Summary

A theoretical analysis for reinforced concrete beams subjected to combined torsion and bending has been presented on the basis of a space truss model. This model consists of the reinforcing cage made up of the longitudinal reinforcement, the stirrups and the concrete compression diagonals acting in the plane of the reinforcement. The analysis is based on the upper and lower bound theorems of the theory of plasticity. In order to insure the formation of a mechanism by yielding of the reinforcing steel limits have been set on the nominal shear stress in the effective concrete shell of the cross section. To avoid local failures the proper detailing of the reinforcement has been indicated.

A comprehensive series of tests ([1] to [4]) has demonstrated the applicability of this analysis to reinforced and prestressed concrete beams with solid, box and T-sections. Part of the findings have already been included in the chapter on torsion of the revised CEB-Recommendations [7].

The research program on torsion at the Institute of Structural Engineering, Swiss Federal Institute of Technology, is financially supported by the Foundation for Scientific Research of the Society of Swiss Cement Manufacturers. The authors would like to express their sincere appreciation for this continuing support.

### Résumé

La résistance à la rupture de poutres en béton armé soumises à la torsion et à la flexion a été analysée sur la base d'un modèle de treillis spatial. Ce modèle consiste d'une cage renforcée constituée des armatures en long, des étriers et des diagonales comprimées en béton qui se forment dans le plan des armatures. La déduction de la charge de rupture s'appuie sur les théorèmes des limites inférieures et supérieures de la théorie de la plasticité. Pour avoir

la certitude de la formation d'un mécanisme par écoulement des armatures, il est proposé de limiter les contraintes nominales de cisaillement dans l'enveloppe efficace du béton. Le détail de la mise en place des armatures devant empêcher des ruptures locales est également indiqué ici.

Un série d'essais choisis ([1] à [4]) a confirmé que cette méthode était applicable à des poutres en béton armé ou précontraint, ayant des sections pleines, des sections en caisson ou en T. La méthode a été introduite en partie dans le chapitre sur la Torsion des Recommandations révisées du CEB [7].

Le programme d'études sur la torsion de l'Institut des Ponts et Charpentes de l'Ecole Polytechnique Fédérale Zurich, est soutenu financièrement par la Fondation pour des Recherches scientifiques de la Société Suisse des Fabricants de Ciments, Chaux et Gypse. Les auteurs tiennent à remercier très sincèrement cette fondation pour son soutien continu.

### **Zusammenfassung**

Der Bruchwiderstand von Stahlbetonbalken unter Torsion und Biegung ist theoretisch auf Grund eines räumlichen Fachwerkmodelles untersucht worden. Das physikalische Modell setzt sich zusammen aus dem durch die Längseisen und Bügel gebildeten Armierungskorb und den Betondruckdiagonalen, welche sich in der Ebene der Armierung ausbilden. Die Herleitung der Bruchlast wird sowohl mit dem unteren wie mit dem oberen Grenzwertsatz der Plastizitätstheorie durchgeführt. Um die Ausbildung eines Mechanismus durch Fliessen der Armierung sicher zu stellen, wird eine Beschränkung der nominellen Schubspannung in der wirksamen Betonschale des Querschnittes vorgeschlagen. Die konstruktive Ausbildung der Armierung zur Vermeidung von lokalen Brüchen ist ebenfalls aufgezeigt.

Eine Serie von ausgewählten Versuchen ([1] bis [4]) hat die Anwendbarkeit dieser Berechnungsmethode auf Stahlbeton- und Spannbetonbalken mit Voll-, Kasten- und T-Querschnitt bestätigt. Zum Teil ist die Methode bereits im Kapitel über Torsion der revidierten CEB-Empfehlungen [7] übernommen worden.

Das Forschungsprogramm über Torsion des Institutes für Baustatik, Abteilung Massivbau, Eidgenössische Technische Hochschule Zürich, wird finanziell durch die Stiftung für wissenschaftliche, systematische Forschungen auf dem Gebiete des Beton- und Eisenbetonbaues des Vereins Schweizerischer Zement-, Kalk- und Gips-Fabrikanten unterstützt. Für diese fortlaufende Förderung möchten die Autoren der Stiftung aufrichtig danken.

Leere Seite  
Blank page  
Page vide